



# Photodynamic effect of Radachlorin on nerve and glial cells



M.A. Neginskaya<sup>a</sup>, E.V. Berezhnaya<sup>a</sup>, M.V. Rudkovskii<sup>b</sup>,  
S.V. Demyanenko<sup>b</sup>, A.B. Uzdensky Ph.D.<sup>b,\*</sup>

<sup>a</sup> A.B. Kogan Research Institute for Neurocybernetics, Southern Federal University, Rostov-on-Don 344090, Russia

<sup>b</sup> Department of Biophysics and Biocybernetics, Southern Federal University, Rostov-on-Don 3440290, Russia

Available online 26 June 2014

## KEYWORDS

Photodynamic therapy;  
Radachlorin;  
Neuron;  
Glial;  
Necrosis;  
Apoptosis

## Summary

**Background:** Radachlorin, a chlorine-derived photosensitizer, is used currently in photodynamic therapy (PDT) of skin cancer. In this work we studied Radachlorin-PDT effect on peripheral nerve and glial cells that are damaged along with tumor tissue.

**Methods:** We used simple model objects – a crayfish stretch receptor that consists of a single sensory neuron surrounded by glial cells and crayfish nerve cord consisting of nerve fibers and ganglia. Radachlorin absorption and emission spectra were registered using spectrophotometer and spectrofluorimeter. Radachlorin accumulation and intracellular localization were studied using the fluorescence microscope. Necrotic and apoptotic cells were visualized using propidium iodide and Hoechst 33342. Neuronal activity was registered using standard electrophysiological methods.

**Results:** Radachlorin absorption spectrum in the physiological van Harreveld saline (pH 7.3) contained maximums at 420 and 654 nm. Its fluorescence band 620–700 nm had a maximum at 664 nm. In the crayfish stretch receptor Radachlorin localized predominantly to the glial envelope and penetrated slightly into the neuron body and axon. Radachlorin rapidly accumulated in the crayfish nerve cord tissue within 30 min. Its elimination in the dye-free solution occurred slower: 11% loss for 2 h. Radachlorin-PDT inactivated the neuron and induced necrosis of neurons and glial cells and glial apoptosis at concentrations as low as  $10^{-10}$ – $10^{-9}$  M.

**Conclusions:** Radachlorin rapidly accumulates in the nervous tissue, mainly in glial cells, and demonstrates very high photodynamic efficacy that characterize it as a promising photosensitizer.

© 2014 Elsevier B.V. All rights reserved.

\* Corresponding author at: A.B. Kogan Research Institute for Neurocybernetics, 194/1 Stachky Ave., NII NK, Rostov-on-Don 344090, Russia. Tel.: +7 8632 433111; fax: +7 8632 433577.

E-mail address: [auzd@yandex.ru](mailto:auzd@yandex.ru) (A.B. Uzdensky).

## Introduction

Photodynamic therapy (PDT) is based on photoinduced generation of strongly cytotoxic singlet oxygen, following oxidative stress and death of stained cells under light exposure in the presence of oxygen. It is currently used in oncology [1–3]. Derivatives of hematoporphyrin (Photofrin II, Photoheme, Hpd), benzoporphyrin (vereporphin), chlorins (mTHPC or Foscan), and 5-aminolevulinic acid (ALA) are the most popular photosensitizers for PDT. However no one of them satisfy all demands for an ideal photosensitizer [4]. Some very efficient photosensitizers are not used in clinics or have only limited applications because of one or two unacceptable parameters. For example, hematoporphyrin derivatives have relatively weak light absorbance in the red spectral region. Aluminum phthalocyanine Photosens retains in the organism for more than two months that imparts too long skin and eye photosensitivity.

Chlorine derivatives have excellent spectral and photochemical parameters. Radachlorin, the mixture of the sodium salts of chlorine e6, chlorine p6 and purpurin 18

(Fig. 1), is a promising photosensitizer. Radachlorin-PDT is adopted for skin cancer treatment in Russia and Korea and showed promising results for treatment of the cervical, gastrointestinal, head and neck, lung and bladder tumors [5–14]. However, in all cancer cases PDT damages not only tumor cells but also nearby peripheral nerve elements and glial cells. It is the most important in the case of treatment of brain tumors, when photodynamic injury of neighboring normal neurons and glial cells can induce unacceptable side effects and neurological disorders. The cellular and molecular mechanisms of photodynamic damage to neurons and glial cells are difficult to study in the brain because of its complexity and numerous intercellular interactions. Biochemical study cannot identify processes that occur separately in different cell types – neurons or glial cells.

The suitable simple object for simultaneous study of interacting neurons and glial cells is the crayfish stretch receptor that consists of a single mechanoreceptor neuron surrounded by a multilayer glial envelope [15]. The photodynamic effects of diverse hematoporphyrin, phthalocyanine,

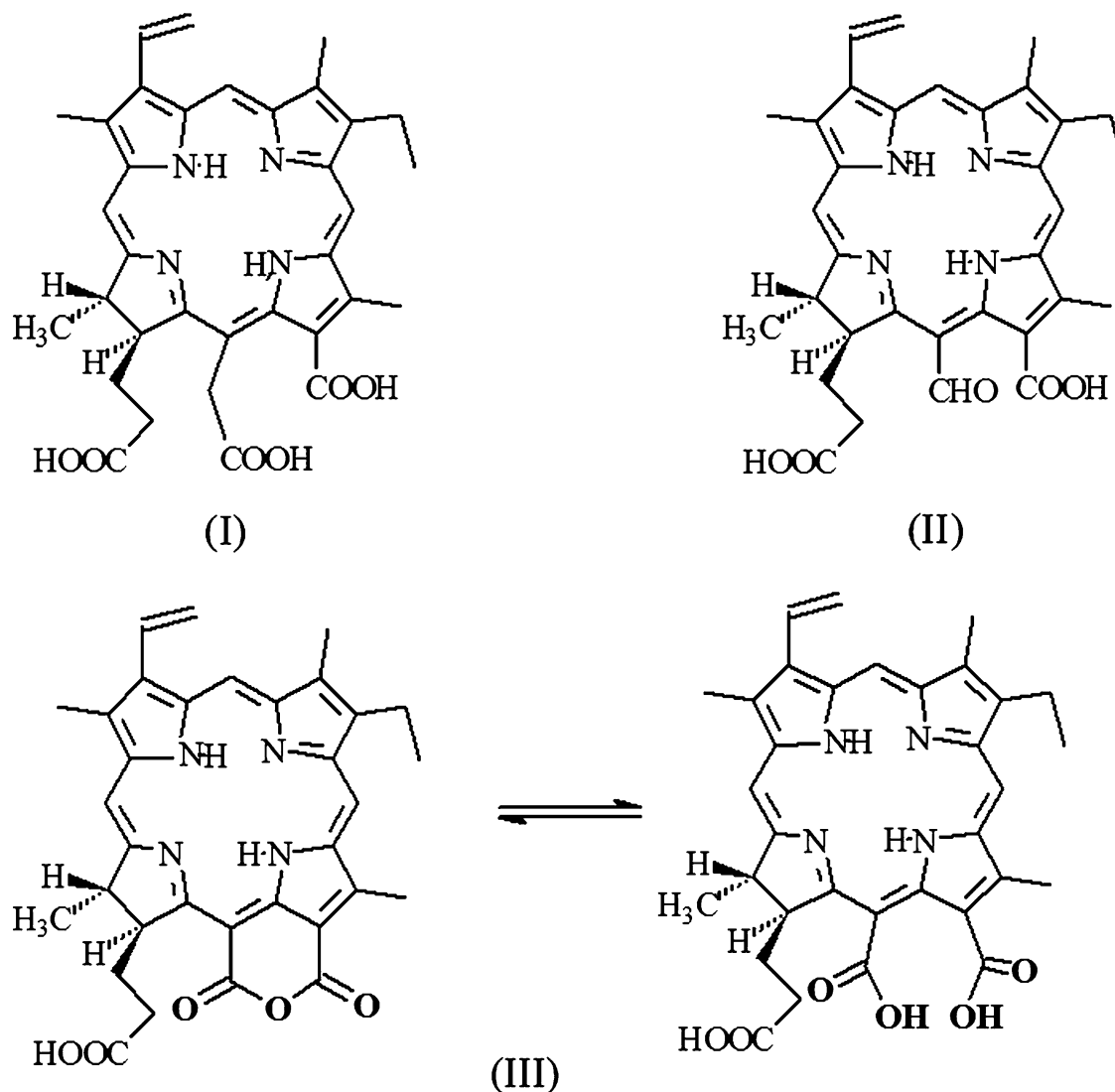


Figure 1 Radachlorin components: chlorine e6 (80%), chlorine p6 (15%), purpurin 18 (5%).

chlorine and hypericin derivatives on the neuronal activity have been earlier studied [1,16–19].

In the present work we studied the effect of Radachlorin-PDT on neurons and surrounding glial cells in the isolated crayfish stretch receptor. We showed that Radachlorin quickly accumulates in the crayfish nervous tissue (abdominal nerve cord) and localizes mainly in the glial envelope surrounding neurons. Radachlorin-PDT inactivates neurons at subnanomolar concentrations and efficiently induces necrosis of neurons, and necrosis and apoptosis of satellite glial cells.

## Materials and methods

### Chemicals

Radachlorin (Fig. 1) was kindly provided by Dr. O.I. Zalevskaya (RadaPharma, Moscow, Russia, [www.radapharma.ru](http://www.radapharma.ru)). Other chemicals were obtained from Sigma–Aldrich-Rus (Moscow, Russia).

### Spectral measurements

The absorption spectrum of the Radachlorin in the physiological van Harreveld saline (pH 7.3) was registered with a SF-2000 spectrophotometer (LOMO, Saint-Petersburg, Russia); the fluorescence spectrum – with a F-4010 spectrofluorimeter (Hitachi, Japan).

### The crayfish stretch receptor preparation and registration of neuronal activity

The crayfishes *Astacus leptodactylus* from Don River affluences were purchased on the local market. Their abdominal stretch receptors were isolated as described in [20]. These were placed into a plexiglass chamber equipped with a device for receptor muscle extension and filled with 2 ml of van Harreveld saline (mM: NaCl – 205; KCl – 5.4; NaHCO<sub>3</sub> – 0.2; CaCl<sub>2</sub> – 13.5; MgCl<sub>2</sub> – 5.4; pH 7.2–7.4). Neuronal activity was recorded extracellularly from axons by the glass pipette suction electrodes. It was then amplified, digitized by the analog-digital converter L-761 (L-Card, Moscow, Russia), and processed by a personal computer using the home-made software that provided continuous monitoring of firing. Experiments were carried out at  $23 \pm 4^\circ\text{C}$ .

### Neuroglial distribution of Radachlorin and its accumulation in the crayfish nerve cord

In order to study the cellular localization of Radachlorin, the isolated crayfish stretch receptor was incubated 10 min in the van Harreveld saline containing  $5 \times 10^{-6}$  M of the sensitizer (Radachlorin molar concentration was assumed to be approximately the same as the concentration of chlorine e6, its major component). Then the dye solution was replaced by the van Harreveld saline and the preparation was photographed with the fluorescence microscope Axiolab.A1 (Carl Zeiss, Germany). The accumulation of Radachlorin in the nervous tissue and following elimination was studied in the crayfish abdominal nerve cord. After isolation, the nerve

cord was weighted and incubated for different time intervals: 1; 5; 15; 30 and 60 min in the Radachlorin solution ( $5 \times 10^{-5}$  M). Then it was washed 3 times with the van Harreveld saline, homogenized in the extraction/labeling buffer (E0655, Sigma–Aldrich Co.), centrifuged 10 min at 15,000 rpm and  $4^\circ\text{C}$ . The fluorescence of the supernatant was registered with a spectrofluorimeter F-4010 (Hitachi, Japan). The Radachlorin elimination was studied in this preparation after 1 or 2 h incubation in the free van Harreveld saline.

### Photodynamic treatment

At the beginning of the experiment the initial level of neuronal activity was set near 8–10 Hz by application of the appropriate receptor muscle extension. After 30-min control recording of neuronal activity, Radachlorin was added into the chamber and after following 30-min incubation, cells were irradiated with the He–Ne laser ( $632.8\text{ nm}$ ,  $0.15\text{ W/cm}^2$ ). 30-min light exposure was longer than the duration of bioelectric neuron response measured from the irradiation start to the moment of firing abolition (typically, 10–20 min), which we called the ‘‘neuron lifetime’’. Radachlorin was present in the chamber during and after the irradiation.

### Cell death assay

In order to visualize dead neurons and glial cells,  $20\ \mu\text{M}$  propidium iodide and  $10\text{--}20\ \mu\text{M}$  Hoechst 33342 were added into the experimental chamber at 8 h postirradiation. This time interval was sufficient for apoptosis development [21]. Then the preparations were washed with van Harreveld saline, fixed with 0.2% glutaraldehyde, again washed and mounted in glycerol. Fluorescent images were acquired using the fluorescence microscope Axiolab.A1 (Carl Zeiss, Germany). Propidium iodide, a membrane impermeable fluorochrome, imparts red fluorescence to the nuclei of necrotic cells with the compromised plasma membrane. Hoechst 33342 imparts blue fluorescence to the nuclear chromatin. It visualizes intact nuclei of living cells and fragmented nuclei of apoptotic cells (Fig. 2). Nucleus fragmentation is the final stage of apoptosis when the no-return point has passed. It should be mentioned that other methods for apoptosis evaluation such as caspase activation, cytochrome c release, or annexin V assay, which require observation of the cytoplasm or the plasma membrane, are unsuitable for study of glial cells in the crayfish stretch receptor because of their multilayer roulette-like morphology and overlapping of optical images of different glial processes and the neuronal cytoplasm [15]. The red nuclei of necrotic glial cells stained by propidium iodide were counted in the predetermined standard field ( $100\ \mu\text{m} \times 100\ \mu\text{m}$ ) around the neuronal soma so that the neuron nucleus was situated in its center. Fragmented nuclei of apoptotic glial cells were counted around the proximal 2 mm axon fragment where the glial apoptosis was more profound. Their mean number representing the level of glial apoptosis was expressed as relative units. Data are presented as mean  $\pm$  S.E.M.

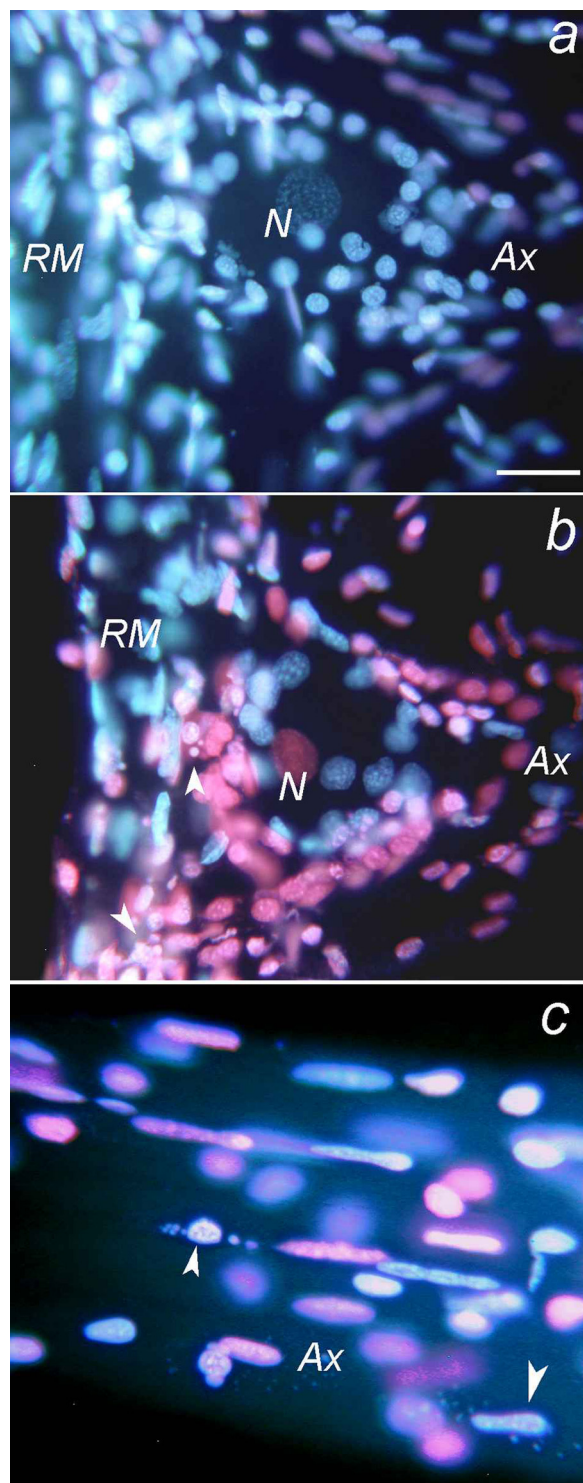


**Figure 2** PDT effect on the isolated crayfish stretch receptor. (a) Control; (b) PDT-treated preparation, the neuronal body region; (c) PDT-treated preparation – the proximal axon fragment. The preparation was fluorochromed with propidium iodide that imparts the red fluorescence to nuclei of necrotic cells and with Hoechst 33342 that imparts blue fluorescence to nuclei of alive or fragmented apoptotic cells. White arrowheads – fragmented nuclei of apoptotic glial cells. RM – receptor muscle; N – neuronal nucleus; Ax – axon. The scale bars – 20  $\mu\text{m}$  at (a) and (b), 10  $\mu\text{m}$  at (c).

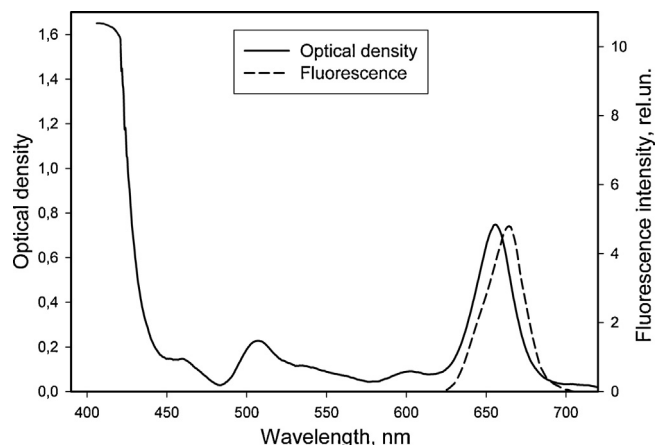


**Figure 3** Absorption and emission ( $\lambda_{\text{ex}} = 420 \text{ nm}$ ) spectra of  $10^{-5} \text{ M}$  Radachlorin dissolved in physiological van Harrevelde saline (pH 7.3).

## Results

### Absorption and fluorescence spectra of Radachlorin

The absorption spectrum of the aqueous Radachlorin solution ( $2 \times 10^{-5} \text{ M}$ ; pH 7.3) contained maximums at 420 and 654 nm (Fig. 3a). The second maximum is specific for chlorines and other chlorophyll derivatives. It corresponds to the “transparency window”, in which red light penetrates deeper through skin into the tissues and acts on deeper structures than the light of other wavelength diapasons.

Radachlorin brightly fluoresces in the red spectral region. Its emission spectrum consisted of the broad band ranging from 620 to 700 nm with a maximum at 664 nm (Fig. 3b).

### Radachlorin accumulation in the crayfish nerve cord and localization in neurons and glia

Radachlorin ( $5 \times 10^{-5} \text{ M}$ ) was accumulated in the isolated crayfish nerve cord tissue mainly within the first 30 min;

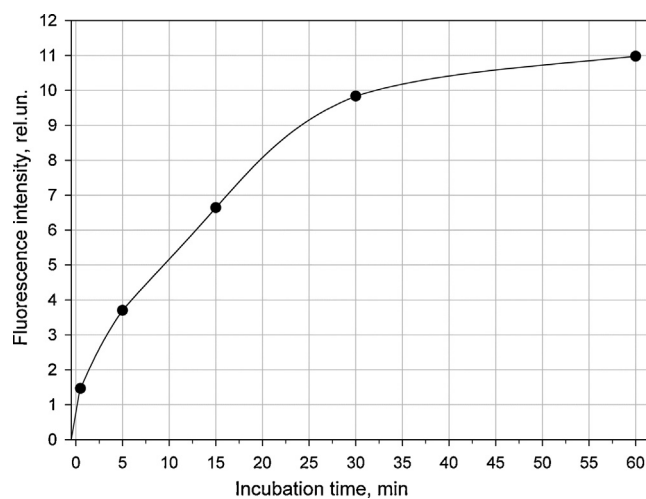


**Figure 4** The dynamics of Radachlorin ( $5 \times 10^{-5} \text{ M}$ ) accumulation in the crayfish nerve cord tissue ( $\lambda_{\text{ex}} = 420 \text{ nm}$ ).

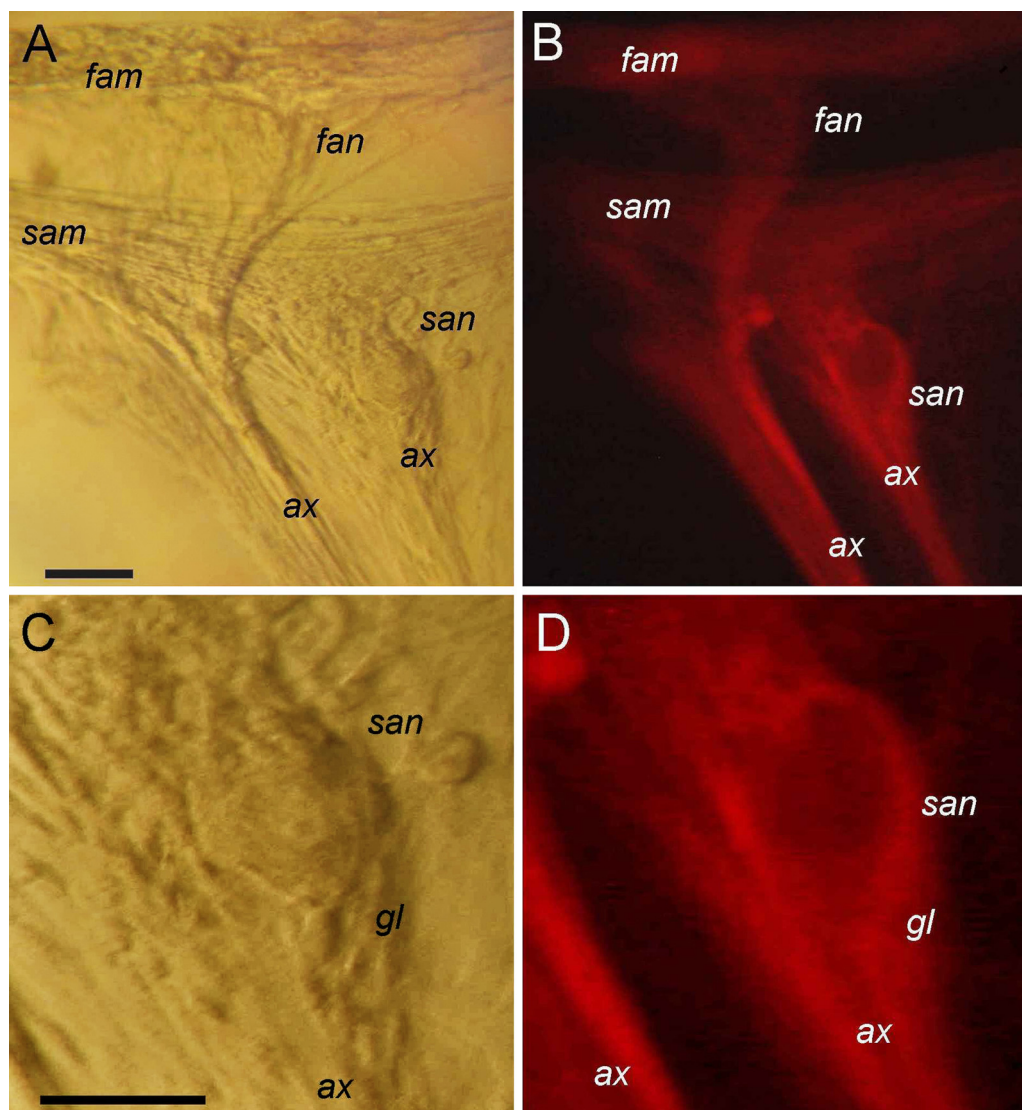


**Figure 5** The distribution of Radachlorin fluorescence in the isolated crayfish stretch receptor (B and D) obtained at low (A and B; 20 $\times$ ) and high (C and D, 40 $\times$ ) magnification. (A and C) – bright field images of the same preparation. *fam* – fast adapting receptor muscle, *sam* – slowly adapting receptor muscle, *fan* – fast adapting mechanoreceptor neuron, *san* – slowly adapting receptor neuron, *gl* – glial envelope, *ax* – axon. Scale bars on (A) – 40  $\mu$ m, on (C) – 50  $\mu$ m.

and during next 30 min its level increased only slightly, by 11% (Fig. 4). It was eliminated slower: only by 11% after 2 h washing off with dye-free van Harreveld saline (Table 1).

After 1 h incubation of the crayfish stretch receptor with  $5 \times 10^{-6}$  M Radachlorin, its fluorescence was concentrated mainly in the glial envelope around the sensory neuron and, to lesser extent, in dendrites and receptor muscles. Radachlorin penetrated only slightly into the neuronal soma and axon. Possibly, it was primarily adsorbed at the surfaces of glial processes that enwrap the neuron (Fig. 5).

#### Radachlorin-PDT effect on neuronal activity

The responses of neuronal firing to photodynamic action of Radachlorin depended on Radachlorin concentration. At the low concentrations ranging from  $5 \times 10^{-11}$  to  $5 \times 10^{-10}$  M firing steadily slowed down until complete and irreversible

**Table 1** Accumulation of Radachlorin in the crayfish nerve cord and elimination in the dye-free solution.

Incubation time (min)	Washing time (min)	Radachlorin fluorescence intensity (rel. un.)
<i>Accumulation</i>		
0.5	–	1.5
1	–	3.0
5	–	3.7
15	–	6.6
30	–	9.8
60	–	11.0
<i>Elimination</i>		
60	60	11.6
60	120	9.8

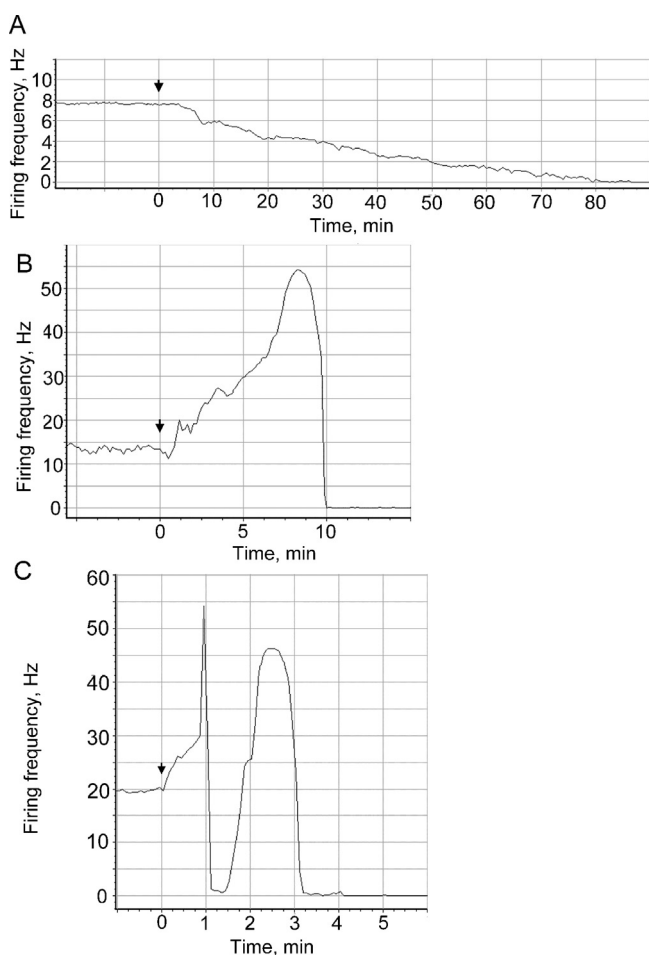


**Figure 6** The typical responses of the crayfish stretch receptor neuron to photodynamic treatment with relatively low (A,  $5 \times 10^{-10}$  M), moderate (B,  $5 \times 10^{-8}$  M) or high (C,  $2.5 \times 10^{-6}$  M) Radachlorin concentrations. Arrows show the start of irradiation.

cessation (inhibitory I-response, Fig. 6A) in 70–80% of the experiments. In approximately 10% of the experiments firing frequency increased, and then neuronal activity rapidly ceased (excitatory E-response, Fig. 6B). In remaining experiments PDT did not influence neuronal activity. At higher concentrations ( $5 \times 10^{-9}$ – $5 \times 10^{-8}$  M) I-responses were observed more rare, in approximately 40% of the experiments; E-responses – in 10%; in 20% of the experiments both, slowly and rapidly adapting neurons consecutively demonstrated the excitatory E-type responses with rapid cessation of firing (EE-response, Fig. 6C), and in remaining experiments the neuron firing did not change. At  $5 \times 10^{-7}$ – $5 \times 10^{-6}$  M Radachlorin-PDT induced EE-responses in 50% of the experiments; in 40% we observed E-responses, and in other experiments firing rapidly stopped. Therefore, intense PDT induced mainly neuron excitation followed by firing block, whereas weak treatment mainly inhibited firing.

Like in the earlier study [19], the concentration dependency of the neuron response duration (neuron lifetime) that determines the PDT intensity:  $T(C)$  could be approximated by the power function:  $T(C) = a \times C^{-b}$  that is linear in the double logarithmic coordinates, where  $a$  and

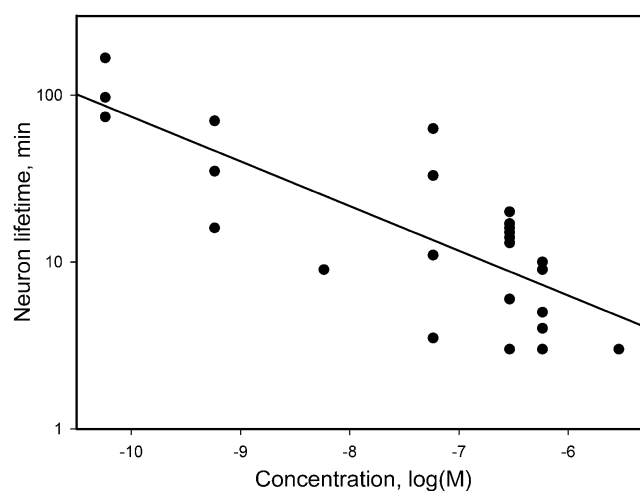


**Figure 7** Neuron lifetime  $T$  (min) versus logarithm of Radachlorin concentration  $C$  (M).

$b$  were determined by the least squares method from Fig. 7:

$$\lg T = -0.74 - 0.26 \lg C,$$

Since this function is not steep ( $b=0.26$ ), the Radachlorin can inactivate neurons at very low concentration range ( $10^{-9}$ – $10^{-7}$  M) for 3–30 min, a reasonable time for PDT application.

### Radachlorin-PDT-induced death of neurons and glial cells

At a concentration of  $2.5 \times 10^{-7}$  M, Radachlorin-PDT inactivated the neuron for approximately 13 min (Fig. 8A) and efficiently induced necrosis of neurons and glia as well as apoptosis of glial cells. At 8 h after such treatment, the level of neuronal necrosis increased from 0% in control to 90% ( $p < 0.001$ ; Fig. 8B), and necrosis of glial cells – from 3 to 70% ( $p < 0.001$ ; Fig. 8D). The level of glial apoptosis also dramatically increased from 2 to 28 relative units ( $p < 0.001$ ; Fig. 8C).

### Discussion

The obtained data showed high photodynamic efficiency of Radachlorin. It well absorbs red light within the “phototherapeutic spectral window” 620–800 nm ( $\lambda_{\max} = 654$  nm), rapidly accumulates in the nervous tissue, and demonstrates phototoxicity at very low concentrations ( $10^{-11}$ – $10^{-9}$  M). These data are in agreement with the earlier observation on its phototoxicity in the subnanomolar concentration range [19]. According to [11], Radachlorin very efficiently produced reactive oxygen species (ROS) after red light (664 nm) exposure.

We observed much higher Radachlorin accumulation in the glial envelope than in the neuronal soma and processes. Glial cells are known to form the roulette-like envelope around the neuron that consists of 10–30 glial layers [15]. Their surface is many times greater than the surface of the

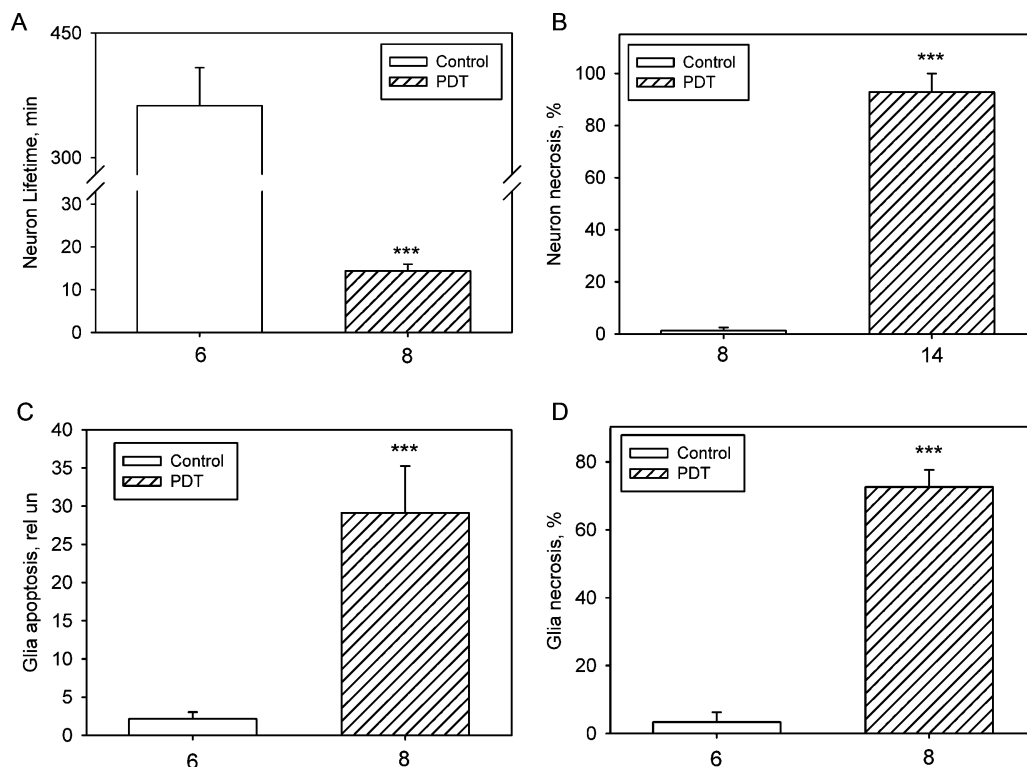


**Figure 8** Effect of Radachlorin-PDT ( $2.5 \times 10^{-7}$  M) on neuron lifetime (A), necrosis of neurons (B) and glial cells (D), and apoptosis of glial cells (C) compared to control preparations. Significant difference from control:  $***p < 0.001$ .

neuron. One can suggest that the hydrophilic Radachlorin components are mainly adsorbed at the cell surface. This could be the reason of higher Radachlorin accumulation in the glial envelope than inside neurons. Since the adsorption process is much faster than the penetration through the cellular membranes, this is also the reason of its rapid accumulation in the nervous tissue and fast elimination after washing off.

In the cultured tumor cells, Radachlorin was also reported to be first adsorbed at the plasma membrane, then diffused inside the cell and accumulated predominantly in the perinuclear endoplasmic reticulum but not in the nucleus [6,10,11]. Unlike the bright cytoplasm fluorescence, it is difficult to register the fluorescence of the thin plasma membrane. In the experiments with the stretch receptor, we could judge on the photosensitizer localization and its site of action not only by the fluorescence distribution but also by PDT-induced changes in the neuronal activity. Bioelectric data clearly indicated that PDT with very small photosensitizer concentration (below  $10^{-10}$ – $10^{-9}$  M) could significantly change the neuronal activity. Photosensitization rapidly disturbs the integrity of the plasma membrane that impairs ionic homeostasis and induces depolarization followed by acceleration of firing, “depolarization block” of neuronal activity and, in the case of sustained irradiation, by necrosis [1,22]. As suggested earlier, such E-response of the stretch receptor neuron was usually caused by intense PDT with a relatively high photosensitizer concentration. In contrast, inhibitory I-responses that were induced by rather weak PDT with relatively low photosensitizer levels were associated

with photodamage of mitochondria and endoplasmic reticulum and release of stored  $\text{Ca}^{2+}$  that inhibits firing through activation of  $\text{Ca}^{2+}$ -dependent  $\text{K}^{+}$ -channels, which hyperpolarize the cell. Intense PDT induces mostly necrosis, whereas apoptotic cell death is usually result of relatively weak but prolonged impact [1,22,23].

A weak dependence of Radachlorin-PDT effect on PS concentration that was characterized with  $b = 0.26$  suggests that one photosensitizer molecule absorbing photon could induce about 4 secondary lesions resulting in firing changes. These might be free radical-induced lipid peroxidation chains damaging the cell membrane [1,16–19].

Radachlorin-PDT also inhibited growth and caused death of cultured cancer cells depending on light intensity [6,11]. Its amphiphilic components form complexes with blood albumins and low density lipoproteins, which deliver them to various tissues within 3–5 h after administration. 98% of Radachlorin excreted from the body or metabolized within 2 days. Patients well tolerate administration of Radachlorin without adverse effects [5,7–11]. The successful use of Radachlorin-PDT for treatment of basal cell skin tumors, cancer of the esophagus, stomach, rectum, and some other types of malignancies has been reported [5–14]. Radachlorin received approval for sale in Russia in 2009 and a conditional approval in South Korea (2008). He is a candidate for Phase III clinical trials in the EU [9].

Thus, the present experiments confirmed high photodynamic efficiency of Radachlorin-PDT. It can eliminate neuronal activity, and cause necrosis of neurons and glial cells, and glial apoptosis at subnanomolar concentrations.

## Acknowledgements

The study was supported by RBFR (grants No. 14-04-00741 and 14-04-32270) and Southern Federal University (grant No. 213.01-24/2013-6). Authors thank Dr. O.I. Zalevskaya (RadaPharma, Moscow) for providing Radachlorin.

## References

- [1] Uzdensky AB. Cellular and molecular mechanisms of photodynamic therapy. Saint Petersburg: Nauka; 2010 (in Russian).
- [2] Agostinis P, Berg K, Cengel KA, Foster TH, Girotti AW, Gollnick SO, et al. Photodynamic therapy of cancer: an update. *CA: Cancer J Clin* 2011;61:250–81.
- [3] Allison RR, Moghissi K. Photodynamic therapy (PDT): PDT mechanisms. *Clin Endosc* 2013;46:24–9.
- [4] Detty MR, Gibson SL, Wagner SJ. Current clinical and preclinical photosensitizers for use in photodynamic therapy. *J Med Chem* 2004;47:3897–915.
- [5] Vakulovskaya EG, Reshetnikov AV, Zalevsky ID, Kemov YV. Photodynamic therapy and fluorescence diagnosis using photosensitizer Radachlorin® in skin cancer patients. *Russ Biother J* 2004;3:77–82 (in Russian).
- [6] Bae SM, Kim YW, Lee JM, Namkoong SE, Han SJ, Kim JK, et al. Photodynamic effects of Radachlorin on cervical cancer cells. *Cancer Res Treat* 2004;36:389–94.
- [7] Markichev NA, Eliseenko VI, Alexeev YV, Arnichev AA. Photodynamic therapy of basal cell skin cancer using chlorine photosensitizers. *Laser Med* 2005;9:23–8 (in Russian).
- [8] Kochneva EV, Privalov VA. Photodynamic therapy in clinical practice. *Laser Med* 2005;9:7–13 (in Russian).
- [9] Kochneva EV, Filonenko EV, Vakulovskaya EG, Scherbakova EG, Seliverstov OV, Markichev NA, et al. Photosensitizer Radachlorin(R): skin cancer PDT phase II clinical trials. *Photodiagn Photodyn Ther* 2010;7:258–67.
- [10] Douillard S, Olivier D, Patrice T. In vitro and in vivo evaluation of Radachlorin (R) sensitizer for photodynamic therapy. *Photochem Photobiol Sci* 2009;8:405–13.
- [11] Douillard S, Lhommeau I, Olivier D, Patrice T. In vitro evaluation of Radachlorin sensitizer for photodynamic therapy. *J Photochem Photobiol B* 2010;98:128–37.
- [12] Hwang H, Biswas R, Chung PS, Ahn JC. Modulation of EGFR and ROS induced cytochrome c release by combination of photodynamic therapy and carboplatin in human cultured head and neck cancer cells and tumor xenograft in nude mice. *J Photochem Photobiol B* 2013;128:70–7.
- [13] Ji W, Yoo JW, Bae EK, Lee JH, Choi CM. The effect of Radachlorin(R) PDT in advanced NSCLC: a pilot study. *Photodiagn Photodyn Ther* 2013;10:120–6.
- [14] Lee JY, Diaz RR, Cho KS, Lim MS, Chung JS, Kim WT, et al. Efficacy and safety of photodynamic therapy for recurrent, high grade nonmuscle invasive bladder cancer refractory or intolerant to bacille Calmette-Guerin immunotherapy. *J Urol* 2013;190:1192–9.
- [15] Fedorenko GM, Uzdensky AB. Ultrastructure of neuroglial contacts in crayfish stretch receptor. *Cell Tissue Res* 2009;337:477–90.
- [16] Uzdensky AB, Derkacheva VM, Dergacheva OY, Zhavoronkova AA. A single neuron response to photodynamic effects of various aluminum and zinc phthalocyanines. *Life Sci* 2000;68:547–55.
- [17] Uzdensky AB, Dergacheva OY, Zhavoronkova AA, Ivanov AV, Reshetnikov AV, Ponomarev GV. Photodynamic effect of deuteroporphyrin IX and hematoporphyrin derivatives on single neuron. *Biochem Biophys Res Commun* 2001;281:1194–9.
- [18] Uzdensky AB, Bragin DE, Kolosov MS, Kubin A, Loew HG, Moan J. Photodynamic effect of hypericin and a water-soluble derivative on isolated crayfish neuron and surrounding glial cells. *J Photochem Photobiol B* 2003;72:27–33.
- [19] Uzdensky AB, Dergacheva OY, Zhavoronkova AA, Reshetnikov AV, Ponomarev GV. Photodynamic effect of novel chlorin e6 derivatives on a single nerve cell. *Life Sci* 2004;74:2185–97.
- [20] Florey E, Florey E. Microanatomy of the abdominal stretch receptors of the crayfish (*Astacus fluviatilis* L.). *J Gen Physiol* 1955;39:69–85.
- [21] Uzdensky A, Kolosov M, Bragin D, Dergacheva O, Vanzha O, Oparina L. Involvement of adenylate cyclase and tyrosine kinase signaling pathways in response of crayfish stretch receptor neuron and satellite glia cell to photodynamic treatment. *Glia* 2005;49:339–48.
- [22] Uzdensky AB, Bragin DE, Kolosov MS, Dergacheva OYu, Fedorenko GM, Zhavoronkova AA. Photodynamic inactivation of isolated crayfish mechanoreceptor neuron: different death modes under different photosensitizer concentrations. *Photochem Photobiol* 2002;76:431–7.
- [23] Uzdensky AB, Zhavoronkova AA, Dergacheva OY. Firing inhibition processes in the response dynamics of isolated crayfish nerve cell to the photodynamic effect of sulphonated aluminum phthalocyanine: participation of free radicals and Ca<sup>2+</sup>. *Lasers Med Sci* 2000;15:123–30.